Journal of Manufacturing Systems 86 (2026) 67–81

Contents lists available at ScienceDirect

Journal of Manufacturing Systems

journal homepage: www.elsevier.com/locate/jmansys

Technical paper

Exploring the core cognitive dynamics of MR-enabled in-situ assembly visualization

Tianyu Liu [a], Weiping He [a,*], Bokai Zheng [a], Jilong Bai [a], Xiaotian Zhang [a], Wenbo Pang [a], Yanli He [a], Mark Billinghurst [b], Lili Wang [c]

[a] Cyber–Physical Interaction Laboratory, Northwestern Polytechnical University, 127 West Youyi Road, Beilin District, Xi'an, 710072, Shaanxi, China
[b] Empathic Computing Laboratory, University of South Australia, Mawson Lakes Blvd, Mawson Lakes, Adelaide, SA 5095, South Australia, Australia
[c] State Key Laboratory of Virtual Reality Technology and Systems , Beihang University, 37 Xueyuan Road, Haidian District, Beijing, 100191, China

ARTICLE INFO

Keywords:
Mixed reality
Blind area assembly
EEG

ABSTRACT

Blind area manual assembly arises from the narrow and inter-obscuring structures of products which makes it difficult for workers to see the assembly site. Mixed Reality (MR) visualization systems can provide intuitive interfaces to improve efficiency and reduce errors in blind assembly, but the neural mechanisms in MR visualization of blind area assembly are not well understood. We conducted a user study (N = 24) that compared the difference in cognitive load between using a future advanced visualization system simulated using MR (Low latency, high accuracy and easy detection of current movements) and blind area assembly with the intention of explaining its core dynamics. Significant differences in electroencephalographic (EEG) features including power spectral density (PSD), coherence (Coh) and event-related potentials (ERPs) were analyzed between the two conditions. And the overall EEG was divided into three segments based on three events (Pickup, Localization and Insertion). The results showed that MR visualization exhibits PSD features such as decreased theta power, increased gamma power, and increased beta power, Coh features such as weakened theta, alpha connectivity, and increased beta, gamma connectivity, and shorter latencies for ERP components such as N2 and P300 at specific phases. We discuss these insights and directions for future work. We hope that research this may provide suggestions for the construction of current blind area assembly visualization systems.

1. Introduction

Manual assembly is an indispensable activity within the field of manufacturing engineering. However, the potential for human error to affect assembly efficiency is a significant concern [1]. This is particularly the case for blind area assembly where the operator's vision is affected by mutual occlusion between assembly parts [2]. Given structural complexity, cost, etc., blind area assembly cannot necessarily be deconstructed into an unobstructed form that provides intuitive assembly training. Mixed Reality (MR) technology can superimpose virtual information onto the real world, offering promising solutions for human–computer interaction in manual assembly processes [3]. Previous studies [4–8] have employed Augmented Reality (AR) to visualize invisible parts, gestures, and other elements in blind areas, thereby enhancing accuracy and efficiency in task performance.

Although using sensors such as cameras to collect blind area information in real time can produce intuitive results [8], but this can also cause problems with hand–eye coordination [4,9] and is difficult to implement in narrow areas. Using tactile sensation or contact force between parts to achieve precise positioning has been proven to be an effective solution [6,10]. This phase is often just before the assembly is finished, and the operator still needs to hold the part in mid-air and find the correct position. However, hand movements and the posture of the part while being held are difficult to track.

MR may be used to overcome some of the limitations of blind area assembly. MR simulation [11] is considered a method that can be used to control experimental variables as a tool for evaluating AR systems that can provide a better field of view(FoV), clarity, etc. In this paper, the obstacles for blind area assembly are addressed by MR simulation, which provides future-proof systems with advanced performance, and it helps us to advise on the development of systems for the present.

MR visualization is generally expressed by means of a virtual model, as its purpose is to mimicking the assembly action in a non-blind area. Considered on a cognitive level, the difference between MR visualization and blind area assembly focuses on the visual representation: the

* Corresponding author.
E-mail addresses: weiping@nwpu.edu.cn (W. He), heyl@nwpu.edu.cn (Y. He).

https://doi.org/10.1016/j.jmsy.2026.02.018
Received 11 June 2025; Received in revised form 31 December 2025; Accepted 20 February 2026
Available online 28 February 2026

virtual model is superimposed in real time on the invisible. Previous studies [12–14] have shown that seeing virtual body movements can trigger similar activation patterns in the brain as viewing real-world scenes. However, operators in blind area assembly cannot see the structures in the real world, and although they can learn from process manuals and perceive the shape through touch and force feedback, their understanding of the blind area assembly is a kind of motor imagery [15]. This means that operators generally do not have a priori experience of actually operating in a blind area. Kinesthetic experience should be valued more than visual representation of movement [9], thus, there could be a difference between MR kinesthetic experience and blind area motor imagery in terms of brain activation patterns. However, this is an area of research that has not been well studied.

In this paper, we explore the impact of MR visualization for blind-area assembly on brain activity, with a specific focus on its role within human-centered manufacturing systems. Rather than targeting the optimization of production equipment or process planning, this work addresses the cognitive and interaction layer of manual assembly, which constitutes a critical yet often underexplored component of digital manufacturing systems.

Compared with previous studies, the main novelty of this work lies in the task-driven integration of an MR-enabled blind-area assembly simulation with Electroencephalography (EEG) analysis, enabling the investigation of how advanced in-situ visualization influences operators' cognitive processes during assembly. By modeling the entire assembly process under MR and analyzing brain activity across key assembly events, this study aims to uncover the influencing factors and core cognitive mechanisms underlying MR-assisted blind-area assembly. The ultimate goal is to establish a cognitive-level understanding of human–computer interaction in assembly tasks, and to provide design-oriented insights that can inform the optimization of human–computer integration in digital manufacturing systems, particularly for precision-demanding, confined-space assembly scenarios requiring real-time feedback. Our contributions include:

1. Creating a MR visualization method integrating gesture tracking and force sensing devices aimed at simulating future advanced blind area assembly MR-enabled systems.
2. Developing a prototype system and conducting a user study to evaluate the system and user experience.
3. Exploring the core dynamics of MR visualization and blind area assembly using EEG analysis and providing some recommendations.

2. Related work

2.1. MR-enabled blind assembly

The concept of MR/AR-enabled blind area assembly was first proposed by Wang et al. [2,16], who highlighted the potential challenges associated with the use of handheld parts or tools in confined or narrow spaces. These limitations, as they relate to the assembly process, stem from the lack of the necessary visual information, which can lead to difficulties or even block the assembly process itself. One of the biggest challenge in AR visualization comes from motion tracking. Khenak et al. [17] compared the difference between visualizing frames or axes for assembled objects in the blind area, however, this may not be applicable for more complex structures as the full model is not shown. There are several examples of MR and AR being used for bland area assembly. Chu et al. [18] built an MR assembly scene and tracked hand movements through Leap Motion sensors and used this to infer the position of parts. They found that when approaching the exact assembly position, the operator tended to locate it by feeling with their fingers. Zhang et al. [5] used data gloves to locate gestures and indirectly calculated the positions of fingertips and parts, but found that using the shoulder position as a reference may cause greater error accumulation. Wei et al. [19] proposed an interactive AR solution for occlusion perception that allows for complete visualization of the part while the hand is occluding it, but this is not applicable when the part is completely occluded. Feng et al. [4] used the position of a head ray to make the target area semi-transparent. In a bolt installation task, they also used hand tracking to indirectly express the position of parts indirectly. The results of their user study indicated an improvement in both learning ability and operational efficiency. In addition, they discussed the method of installing a mini camera on the hand to provide a third-person perspective. Although this improved efficiency in some cases, the lack of incoordination between hand movements and video images brought great difficulties to the operator. Hou [8] et al. focused on providing dynamic status monitoring based on RGBD data, making the system more applicable. Zheng et al.'s [20] work focuses with recognizing arms and guidance, but this also requires the deployment of tracking sensors.

However, the sensor devices used in the above-mentioned AR systems will take up additional space, and the use of wearable devices such as data gloves raise bring about the problem of inaccurate positioning. One solution for this problem is to use force feedback for positioning near the assembly completion stage, which makes full use of the assembly scene itself and conforms to the operator's intuition. In the work of Zhang et al. [6], the effectiveness of applying force sensing devices has been verified, but the gestures were not fully tracked. In this paper, we aim to improve system performance that is currently unattainable by integrating devices such as MR, force sensing and haptics for blind area assembly visualization that is as complete and accurate as possible.

2.2. Perception of virtual movements

The hands and arms are the main parts of the users in the assembly action and are our concern and so we wanted to focus on the perception of virtual movements of these body parts. Our research compares of blind area assembly with MR visualization, using EEG features encompassing cognitive workload [21], attention [22], stress [23], and emotion [24]. These are widely used to measure user experience during human–computer interaction, but also to focus on their core difference: the EEG patterns of real-time action virtual projection and visual-guidance-free operation. Previous work [12,25,26] has shown that motor training in virtual reality produces similar positive effects as real-world training. Motor neurons are modulated by visual information [27], and motor errors in vision can affect motor learning [28,29].

Perani et al. [30] compared the effects of observing virtual movements and real movements on brain perception. They found that only real movements can activate the visual spatial network, otherwise, it only starts the visual perception process. However, they only studied passive observation of movements, rather than actively moving real hands or virtual hands. Daniel et al. [31] investigated simultaneous haptic stimulation of human hidden real and virtual hands, pointing out that subjective illusions of virtual hand ownership can also be induced by imagining motor behavior following virtual hand movements. Through their study of the threat of virtual hands, Gonz'alez-Franco et al. [32] noted that when individuals develop the illusion of ownership of a virtual body, there is an autonomic response that corresponds to what is observed in events that occur in reality. Alimardani et al. [33] pointed out that in hand motor imagery, visual observation similar to real hands optimizes information integration in the brain, thereby providing a sense of embodiment. Silvia et al. [34] compared the differences in executing hand movements from a first-person view in reality, a VR scene showing realistic virtual hands, and a VR scene showing abstract virtual hands. They found using realistic hand models can evoke comparable lateralized activation patterns in motor brain areas than in real-world scene.

More features of virtual hand movements also influence the interaction process, Tieri et al.'s [35] data suggests that limb discontinuity alters the ownership and agency of the virtual body as observed by the individual's first-person perspective, even without any multi-sensory

stimulation of the real body. However, this does not mean that the virtual hand needs to be made more realistic, and the work of Ferran et al. [36] demonstrates that the sense of agency is stronger for less realistic virtual hands, and that the greater sense of ownership of the human virtual hand benefits from the direct mapping between real and virtual hand degrees of freedom. Avinash et al. [37] point out that speed is an important component in combining hand movements with visual and proprioceptive information during interaction with real and virtual objects. Schwind et al. [38] investigated the effect of hand appearance on how the brain combines visual and tactile signals using a cue-conflict paradigm. They show that deviations of virtual hand appearance from human norms affect haptic experience, but do not systematically affect performance on discrimination tasks.

Unlike previous work, our study is driven by the assembly task and analyzes the virtual visualization behavior individually in segments based on haptic and force characteristics.

2.3. EEG analysis in assembly

Most of the previous studies on EEG-assisted assembly have only considered relatively single EEG features. Xiao et al. [39] presented a method for assessing brain fatigue in operators during manual assembly processes, using power spectral density(PSD) as the primary test indicator. Similarly, Kosch et al. [40] help assess cognitive load by measuring alpha power. Pušica et al. [41] also recorded frontal theta and parietal alpha power to assess assembly work. Qin et al. [42] presented a method for assessing brain load in timber frame assembly in which PSD measurements were applied. They [43,44] also proposed methods for categorizing and predicting cognitive load. Morton et al. [45] found that a lower individual alpha frequency (IAF) served as a marker to distinguish between different levels of cognitive load and overload. Alessa et al. [46] measured PSD in the theta, alpha, and beta frequency bands to evaluate cognitive processing workload in assembly. Mijović et al. [47] focused on the event-related potential (ERP) amplitude of the P300 component in the assembly task.

There are also studies in the field of human–computer collaboration that apply EEG. Mohammed et al. [48,49] extracted frequency domain signal features from EEG to generate robot control commands for supporting collaborative human–robot assembly. Their research [50] outlines EEG feature extraction and classification methods in human–computer collaboration. Buerkle et al. [51,52] also uses a similar approach to predict human movement to improve the safety of human-connection collaboration. Wang et al. [53] also classified assembly commands by categorizing time–frequency features.

In summary, the various measures of EEG have yet to achieve greater potential in the cognitive assessment of assembly tasks, and in this work we have attempted to analyze the scenario of blind-area assembly in a more detailed and comprehensive manner.

3. Methods

3.1. MR simulation system

The MR simulation approach has been shown to be an effective strategy for modeling advanced and non-existent systems. AR interface design [54], task training [55], and experiential evaluation [56] all demonstrate the benefits of using an MR simulation approach.

We created the MR visualization system shown in Fig. 1, where hand movements are tracked and displayed optically by MR head mounted display (HMD), assembly scenarios are positioned by the controller, and bolts are positioned by fingertip pressure sensors before touching the product and a 6-axis force sensor when touching the product. The entire scene is shown in MR HMD with the pass-through background, and in order to have better performance we by re-configured the blind area system into an open structure for easy tracking and localization.

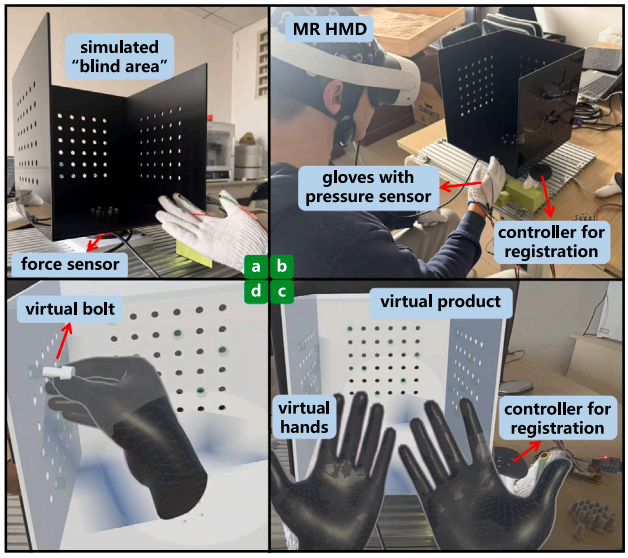

Fig. 1. Simulated "blind assembly" visualization system.

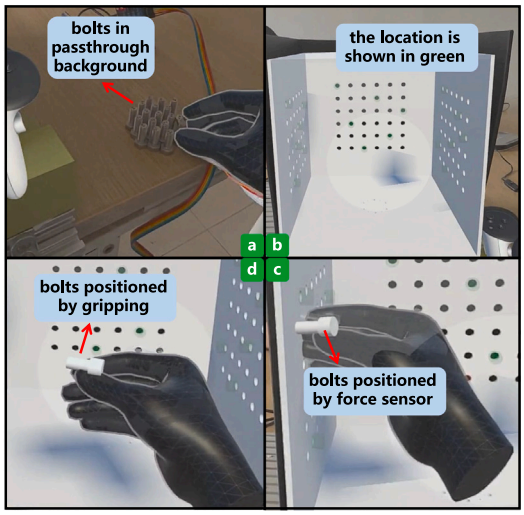

Fig. 2. Assembly process under MR system.

Using a black box as a product the user task involved inserting bolts into holes in the box. This has previous been shown to be a validated and effective scenario [6]. The setup of the system will be described next in terms of a complete one-shot insertion process: finding and picking up the bolt, feeding it into the blind area, finding the target location and confirming and inserting it.

3.2. Assembly task scenario

The entire background environment is shown in pass-through video. Firstly the bolts are neatly lined up next to the product, and participants see through the pass-through(see Fig. 2a), with the user's hand displayed as a virtual model. The blind product is displayed as a virtual model, and the target bolt location is shown in green(Fig. 2b). Participants are asked to pinch the bolt and are given a model of the bolt unobstructed by their hand (Fig. 2c). After the participants take the bolt behind the corresponding hole and made contact, the bolt is converted to a visualization via force feedback is provided to enable more accurate positional tracking (Fig. 2d).

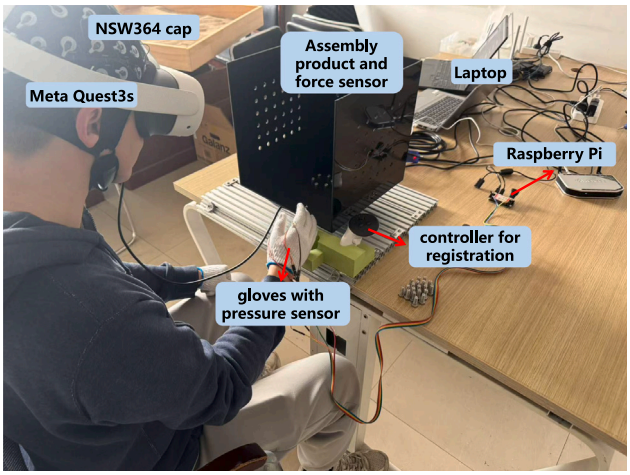

Fig. 3. Hardware setup.

3.3. Hardware and software

Our system integrates multi-sensor fusion, combining optical, tactile, and force feedback data streams. The prototype system used a Meta Quest3s HMD [57] with an LCD display, a resolution of 1832 × 1920 pixels per eye and an 89° diagonal FoV, 90 Hz refresh rate. The VR headset was connected via a USB-C cable to a laptop with the following specifications: AMD Ryzen 7 5800H Core, NVIDIA GeForce RTX 3060 Laptop GPU, 16 GB DDR4 Quad Channel DDR4 memory, 512 GB SSD. The operating system was Windows 11 x64. The force sensing device used was a DECENT γ 74 6-axis force sensor [58] with a measurement range of 3 to 100 Nm and an accuracy of 0.2% full scale. The black box was made of acrylic sheets and weighed 2.8 kg, while the metal bolt weighed 10 g. The fingertip-set thin-film pressure sensor was 0.3 mm thick, with a range of 0 to 500 g with a response point of less than 20 g, and transmits signals to a PC via a Raspberry Pi zero 2 W. We used the NSW364 [59], a 64-channel EEG device with a 10–10 international standard lead system, and we set the sampling frequency to 500 Hz. Fig. 3 shows the entire hardware setup. The software system was made in unity 6000.0.27f1 and each function was developed in C# script. The controller positioning and gesture recognition features were supported through the Meta XR All-in-One SDK [60].

4. User study

4.1. Research question

RQ1: What are the perceptual and performance advantages of using MR visualization in situ guidance in blind assembly?

RQ2: How does MR visualization work with brain cognitive processes in blind assembly?

4.2. Research hypotheses

H1: perceived usability. MR visualization of in situ guidance improves system usability for blind assembly.

H2: task performance. MR visualization of in situ guidance improves user assembly speed and reduces errors in blind assembly.

H3: cognitive load. Cognitive load on the brain is reduced with in-situ guidance of MR visualization of blind assembly.

H4: event impact. Specific event occurrences significantly influence brain cognitive processes in MR visualization of in-situ guidance for blind assembly.

Table 1
Interview questions.

No.	Interview question
Q1	Can you describe your overall experience using the MR visualization system for the assembly task?
Q2	In what ways did the MR visualization make the task easier or more challenging compared to the traditional method?
Q3	Were there any specific features of the MR system that you found particularly helpful or distracting?
Q4	How did the integration of gesture tracking and haptic feedback influence your interaction with the system?
Q5	Did you experience any technical issues or discomfort while using the MR headset or other equipment?
Q6	From your perspective, what are the main advantages and disadvantages of using MR for blind area assembly?
Q7	If you were to use this system in a real-world assembly scenario, what improvements would you suggest to make it more effective?

4.3. Task design

We set up two conditions for user study:

Baseline condition: the participants had to complete the blind area assembly task following a guidance document, where the perspective view of the product model and the target location were provided as paper documents.

MR condition: the participants had to complete the blind area assembly task in a MR view. During the process participants wore MR HMD with their hand and the product presented as virtual models, bolts were similarly displayed as they were pinched out and touched the product surface, and unused bolts were displayed through the pass-through background. Semi-transparent bolt models are shown at all target locations to guide the user.

Participants completed an 18-bolt insertion task in each of the two conditions and were asked to ensure that the bolts were assembled correctly, and were informed of the results only after the task was completed, as shown in Fig. 4.

4.4. Participants

We recruited 24 people, including 18 students and 6 assembly workers(13 male, 5 female), aged 22 to 32 years (M = 26.17, SD = 3.11). All participants were right-handed. Their vision is normal or corrected to normal and they do not have visual diseases or disorders such as color blindness. Of the participants, 20 were familiar with AR interfaces, providing a rating of three or higher on a 5-point Likert item (1: novice, 5: expert). This indicated that they were familiar with AR technology and our results would not be affected by the novelty of the technologies.

4.5. Procedure

A within-subjects user study was conducted with the two conditions mentioned above: Baseline condition and MR condition. The sequences were counter-balanced to avoid learning effects.

Participants filled out demographic questionnaires during the pre-experiment phase, and their training included an introduction to the system setup, task requirements, and usage. In the experiment, participants were asked to sit down, complete tasks in both conditions, and wore an EEG cap at all times. Participants were asked to rest with their eyes closed for 90 s before the task to establish a baseline of brain activity. After completing each condition, participants completed the corresponding questionnaires, and at the end were given a gift valued at $10. The entire experiment lasted approximately 1 h for each participant. In the final interviews we asked the following questions, as shown in Table 1.

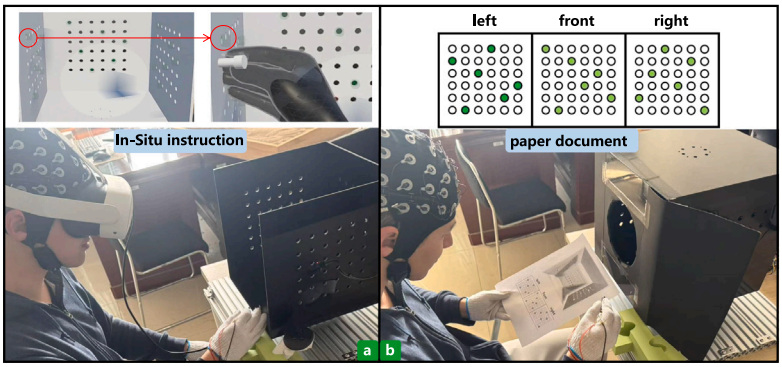

Fig. 4. Assembly conditions. (a)The in-situ instruction is shown in green under MR condition. (b)Blind assembly following the paper document under baseline condition.

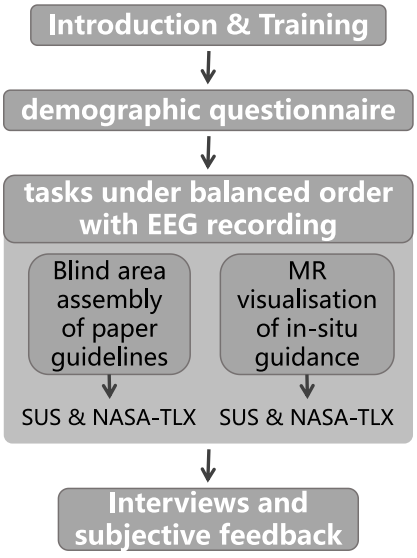

Fig. 5. Experiment procedure.

4.6. Metrics

The demographics questionnaire included a few questions (i.e. name, age, and gender identity). The post-experimental questionnaires were SUS questionnaire, NASA-TLX questionnaire and user preference questionnaire which were used to confirm the performance of the system. We also recorded task completion time and assembly correctness as objective data. The force sensor can detect whether a bolt is inserted in the correct position. We identify errors by comparing this with the preset correct position. Fig. 5 shows the experiment procedure.

Throughout the experiment, we collected EEG data using the NSW cap, measuring the prefrontal (FP1, FP2), inferior frontal(F7, F8), frontal (F3, F4), central (C3, C4), parietal (P3, P4), occipital (O1, O2), temporal (T3, T4), and posterior temporal (T5, T6) lobes. Fig. 6 shows the map of electrode distribution without REF and GND electrodes. The force and pressure sensors were used for precise monitoring of three actions: picking up a bolt, contacting the product for positioning and completing the insertion of the bolt.

For the processing of EEG data we analyzed three features: The assembly process is divided into three phases according to different ERP trigger events, as shown in Fig. 7.

Table 2
Mean (standard deviation) of the SUS results.

	Learnability	Usability	Total
Baseline	70.21(13.49)	64.71(14.20)	66.15(9.89)
MR	64.58(13.63)	82.29(10.57)	78.75(7.84)

Power Spectral Density (PSD): δ (1–3 Hz), θ (4–7 Hz), α (8–11 Hz), β (12–30 Hz), and γ (31–45 Hz), reflecting frequency domain features that help to reveal differences in the brain's functional patterns under different tasks or states.

Coherence (Coh): the degree of synergistic activity between different regions of the brain, reflecting spatial domain features and helping to reveal how brain regions work together to achieve effective information processing and behavioral control.

Event-related potentials (ERPs): changes in EEG signals associated with a specific event, reflecting time-domain features and reflecting the neural activity of the brain at different stages in processing the event. The ERP trigger is based on three key actions and is the same in both conditions.

5. Results

5.1. System performance

The SUS results, NASA-TLX results, task performance and user preferences were first tested to verify the validity of the proposed prototype system.

The SUS results are shown in Table 2 and Fig. 8. For the SUS learnability score, the difference between the baseline and MR conditions was small and not significant, with a Cohen's d of 0.34 (95% CI [−0.07, 0.75]). For the usability score, the MR condition scored significantly higher ($Z = -3.275$, $P < 0.05$, Cohen's $d = -0.96$, 95% CI [−1.44, −0.47]), with a large effect size. Similarly, the total SUS score showed a large improvement ($Z = -3.261$, $P < 0.05$, Cohen's $d = -0.93$, 95% CI [−1.41, −0.45]) for the MR condition.

The average task completion time for the baseline condition was 923.2s, while for the MR condition it was 287.9s (see Fig. 9). The Kolmogorov–Smirnov tests showed that the task completion times in both cases conformed to a normal distribution, and the t-tests indicated that the task completion times for the MR condition were significantly lower ($T=9.108$, $P < 0.01$, Cohen's $d = 2.04$, 95% CI [1.50, 2.55]) than for the baseline condition.

The average number of errors was 0.5 for the baseline condition and 0 for the MR condition (see Fig. 9). The Wilcoxon signed-rank

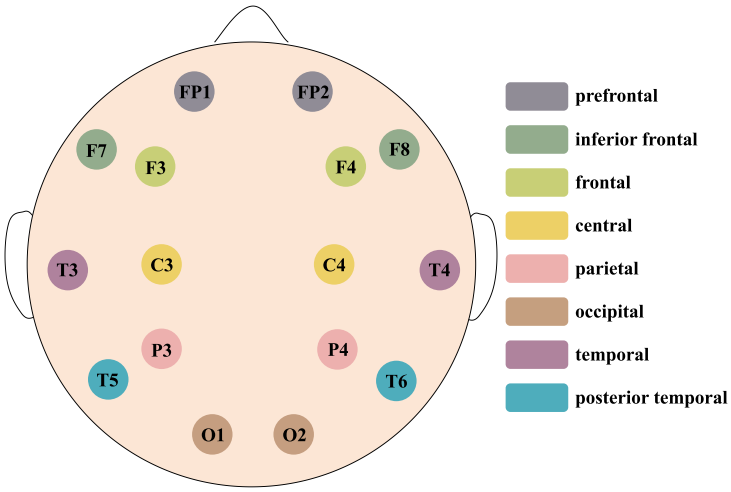

Fig. 6. EEG map.

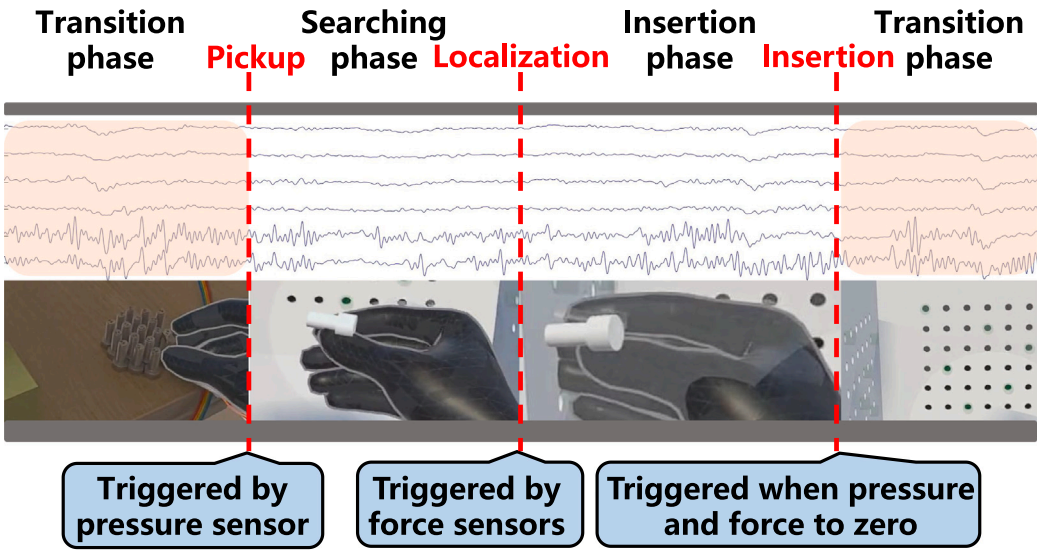

Fig. 7. Phase division.

test showed that the number of errors in the MR condition was significantly less than the baseline condition($Z = -2.070$, $P < 0.05$). And all participants indicated that they preferred the MR visualization system.

The NASA-TLX results are shown in Table 3 and Fig. 10. The Mental Demand ($Z = -3.887$, $P < 0.01$, $r = -0.79$), Physical Demand ($Z = -2.967$, $P < 0.05$, $r = -0.61$), Temporal Demand ($Z = -3.380$, $P < 0.01$, $r = -0.67$), Performance ($Z = -2.101$, $P < 0.05$, $r = -0.43$), Frustration ($Z = -4.286$, $P < 0.01$, $r = -0.87$), and Total scores ($Z = -4.286$, $P < 0.01$, $r = -0.87$) were all significantly better in the MR condition than in the baseline condition. The Effort score showed no significant difference.

When asked about which system they referred using, all participants indicated that they preferred the MR visualization system. In the above tests, the paired data with significant differences all have effect sizes exceeding medium effects (Cohen's $d > 0.5$ or $r > 0.3$). These results show that our prototype system has significant advantages in terms of perceived ease of use, task performance, perceived workload and user preferences.

5.2. EEG analysis

EEG data were recorded using a 64-channel wireless system (NSW364, Neuracle) with electrodes placed according to the international 10–10 system (sampling rate: 500 Hz). Preprocessing was performed offline in MATLAB (R2021b, EEGLAB v2023). Data were band-pass filtered at 1–45 Hz and notch-filtered at 50 Hz, and re-referenced to the common average. Event triggers were defined for three actions: Pickup (fingertip pressure > 20 g), Localization (6-axis force > 0.2 N), and Insertion (sensor values return to baseline). Data were epoched from –500 to 1500 ms relative to triggers, with –200 to 0 ms used for baseline correction.

PSD estimates were obtained on artifact-free data using Welch's method (MATLAB pwelch). For each participant and condition, epochs were either averaged per epoch and then averaged across epochs or concatenated across trials to increase spectral stability. Functional connectivity was estimated using magnitude-squared coherence (MSC) derived from cross-spectral density estimates via Welch's method (MATLAB mscohere/cpsd).

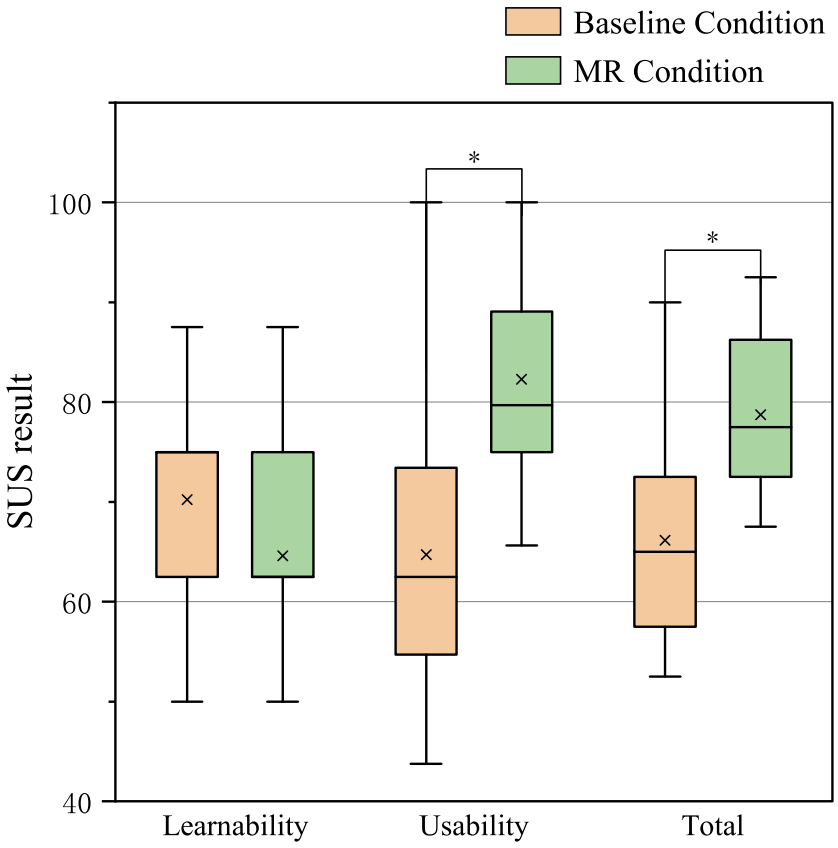

Fig. 8. SUS results.

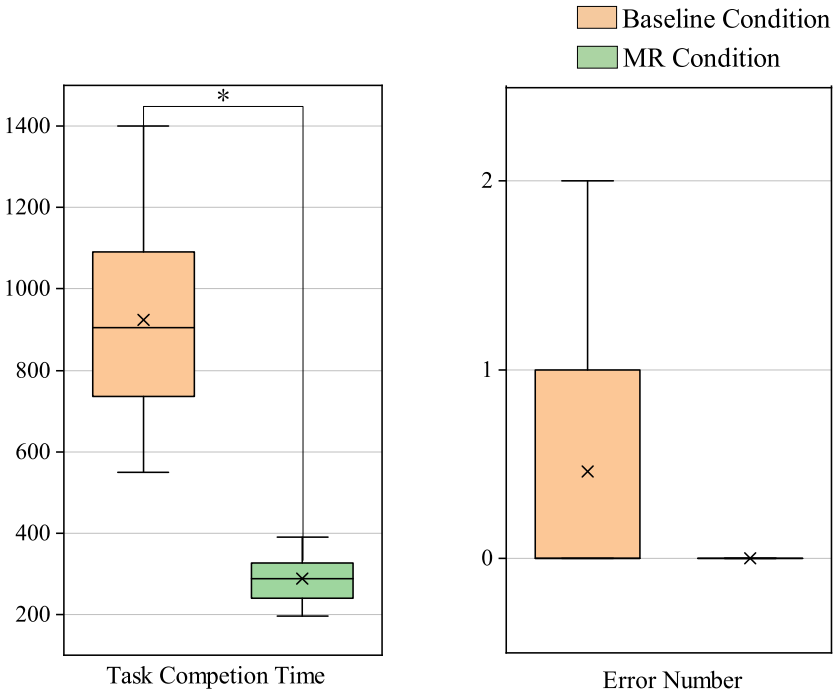

Fig. 9. Task performance.

All data were judged by the Kolmogorov–Smirnov test to determine whether or not they obeyed a normal distribution, t-tests were performed for those that obeyed a normal distribution, and Wilcoxon signed rank tests were performed for those that did not obey for significance. Given a full understanding of the similarities between the two scenarios, we also performed an equivalence test for the PSD, using an empirical equivalence constraint with a significance level of 5% [61]. To address multiple comparisons across electrodes, frequency

Table 3
Mean (standard deviation) of the NASA-TLX results.

	Mental Demand	Physical Demand	Temporal Demand	Performance
Baseline	83.33(8.61)	80.92(8.31)	86.25(6.25)	66.25(10.58)
MR	64.17(10.66)	71.46(11.65)	75.54(10.73)	58.46(10.92)
	Effort	Frustration	Total	
Baseline	41.21(13.43)	70.13(12.07)	74.34(5.77)	
MR	36.42(9.97)	37.46(8.66)	54.36(4.67)	

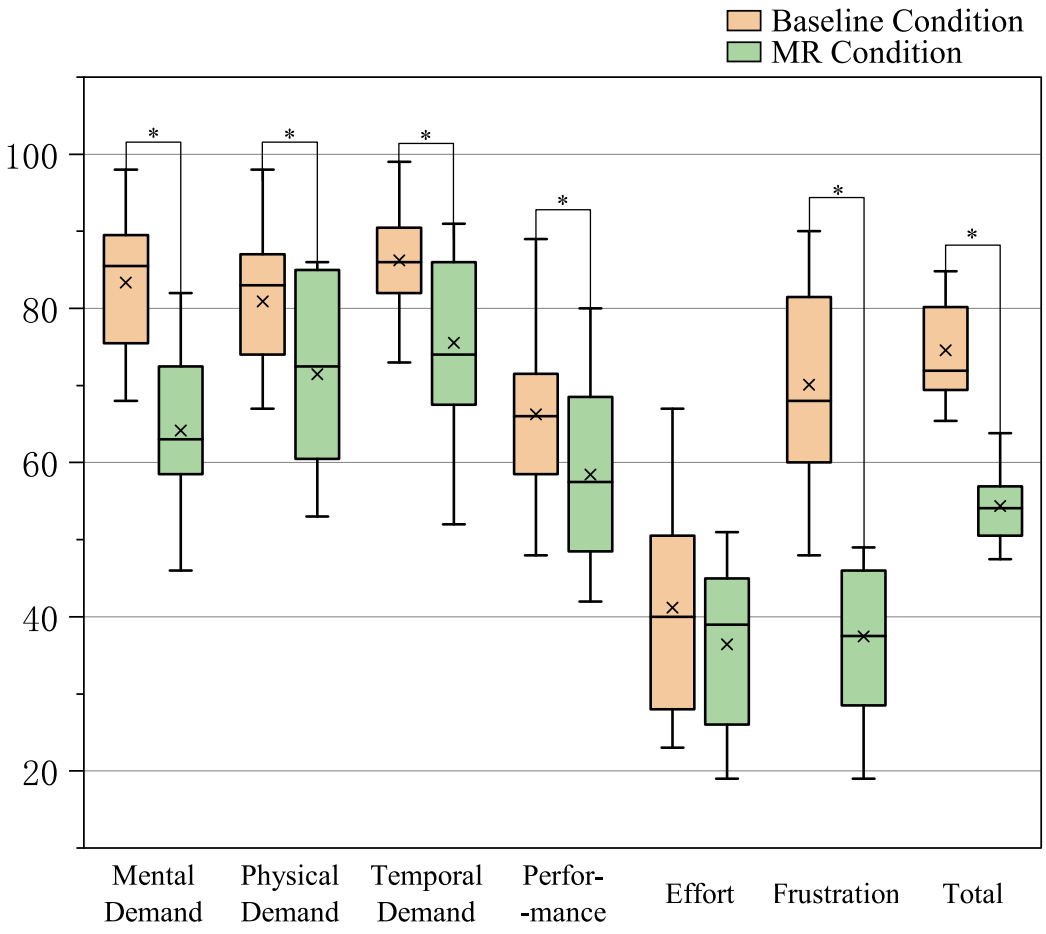

Fig. 10. NASA-TLX results.

bands, and time windows, p-values were adjusted using false discovery rate (FDR, q < 0.05).

During the transition phase, the PSD results for the MR condition relative to the baseline condition are shown in Table 4. The prefrontal (FP1, FP2) and inferior frontal (F7, F8) regions exhibited decreased θ power ($p < 0.05$). In the frontal region (F3, F4), θ power significantly increased ($p < 0.05$). The α power in the center region (C3, C4) shows equivalence. The parietal region (P3, P4) showed a significant increase in β power ($p < 0.05$). In the occipital region (O1, O2), α power significantly decreased ($p < 0.01$). The temporal region (T3, T4) showed decreased α power ($p < 0.05$). No significant changes were observed in the posterior temporal region (T5, T6).

During the searching phase, the PSD results for the MR condition relative to the baseline condition are shown in Table 5. In the prefrontal region (FP1, FP2), θ power significantly decreased ($p < 0.01$) and γ power increased ($p < 0.05$). In the inferior frontal region (F7, F8), α decreased ($p < 0.05$). The frontal region (F3, F4) showed increased β power ($p < 0.05$). In the central region (C3, C4), α and β power decreased ($p < 0.05$). In the parietal region (P3, P4), α power significantly decreased ($p < 0.05$) while γ significantly increased ($p < 0.05$). The occipital region (O1, O2) showed no change in δ, while α significantly decreased ($p < 0.05$) and γ increased ($p < 0.05$). In the temporal region (T3, T4), θ decreased ($p < 0.05$). The posterior temporal region (T5, T6) showed an increase in γ power ($p < 0.05$).

During the insertion phase, the PSD results for the MR condition relative to the baseline condition are shown in Table 6. In the prefrontal region (FP1, FP2), θ power decreased ($p < 0.05$) and β power increased ($p < 0.05$). The frontal region (F3, F4) exhibited increased β power ($p < 0.05$). The central region (C3, C4) showed equivalence in δ, while β power significantly increased ($p < 0.01$) and γ power increased ($p < 0.05$). In the parietal region (P3, P4), α decreased and both β and γ power increased ($p < 0.05$). In the occipital region (O1, O2), γ increased ($p < 0.05$), α decreased. The temporal region (T3, T4) showed equivalence in α power. Finally, the posterior temporal region (T5, T6) exhibited increased γ power ($p < 0.05$).

The Coh results for the MR condition relative to the baseline condition are shown in Fig. 11. The three phases have similar trends: partial connectivity decreases for δ, θ and α, and partial connectivity increases for β and γ (q < 0.05). Specifically, there was less significant change in connectivity in δ, a significant decrease in connectivity between the

Table 4
PSD for the transition phase. $**< 0.01, *< 0.05$, ≡ equivalence.

Brain Region	δ	θ	α	β	γ
prefrontal (FP1, FP2)	–	$*\downarrow$	–	–	–
inferior frontal(F7, F8)	–	$*\downarrow$	–	–	–
frontal (F3, F4)	–	$*\uparrow$	–	–	–
central (C3, C4)	–	–	≡	–	–
parietal (P3, P4)	–	–	–	$*\uparrow$	–
occipital (O1, O2)	–	–	$**\downarrow$	–	–
temporal (T3, T4)	–	–	$*\downarrow$	–	–
posterior temporal (T5, T6)	–	–	–	–	–

Table 5
PSD for the searching phase. $**< 0.01, *< 0.05$, ≡ equivalence.

Brain Region	δ	θ	α	β	γ
prefrontal (FP1, FP2)	–	$**\downarrow$	–	–	$*\uparrow$
inferior frontal(F7, F8)	–	–	$*\downarrow$	–	–
frontal (F3, F4)	–	–	–	$*\uparrow$	–
central (C3, C4)	–	–	$*\downarrow$	$*\downarrow$	–
parietal (P3, P4)	–	–	$*\downarrow$	–	$*\uparrow$
occipital (O1, O2)	≡	–	$*\downarrow$	–	$*\uparrow$
temporal (T3, T4)	–	$*\downarrow$	–	–	–
posterior temporal (T5, T6)	–	–	–	–	$*\uparrow$

Table 6
PSD for the insertion phase. $**< 0.01, *< 0.05$, ≡ equivalence.

Brain Region	δ	θ	α	β	γ
prefrontal (FP1, FP2)	–	$*\downarrow$	–	$*\uparrow$	–
inferior frontal(F7, F8)	–	–	–	–	–
frontal (F3, F4)	–		–	$*\uparrow$	–
central (C3, C4)	≡	–	–	$**\uparrow$	$*\uparrow$
parietal (P3, P4)	–	–	$*\downarrow$	$*\uparrow$	$*\uparrow$
occipital (O1, O2)	–	–	$*\downarrow$	–	$*\uparrow$
temporal (T3, T4)	–	–	≡	–	–
posterior temporal (T5, T6)	–	–	–	–	$*\uparrow$

prefrontal lobe and regions of the lateral frontal and temporal lobes in θ, a significant decrease in connectivity between the occipital lobe and regions of the parietal lobe, posterior temporal lobe, and central lobe in α, a significant increase in connectivity between the frontal lobe, parietal lobe, and central lobe and the frontal lobe to each other in β, and a significant increase in connectivity between the parietal lobe and regions of the occipital lobe and prefrontal lobe in γ.

The ERP features are first segmented according to different time windows [62,63]. Fig. 12 shows the topography of the time-segmented average voltage distribution of the three triggering actions(Pickup, Localization, and Insertion), with a small difference between the two conditions during the baseline period (−200 to 0 ms). For the Pickup trigger event, FP1 electrode in the baseline condition showed positivity during multiple window periods. In the MR condition, electrodes such as FP1, T4 showed positivity in the early period (60–150 ms and 150–200 ms), followed by positivity in electrodes such as C3, C4, P3, P4, and T6. For the Localization trigger event, electrodes such as F4, P4, and T5 in the baseline condition showed positivity over multiple window periods, whereas the FP1 electrode in the MR condition showed positivity. For the Insertion trigger event, electrodes such as T5 and T6 in the baseline condition showed positivity, while F3, F4, and C3 electrodes in the MR condition showed positivity.

Typical components identified by independent component analysis (ICA) for each event are shown in Fig. 13. The Pickup event was prolonged in the MR condition with FP1 producing P300 and C3 and C4 showing P2, while the baseline condition had an N2 component at F3 and T6. The Localization event was prolonged in the MR condition with FP1 showing P2 and P300, again delayed compared to F4 and P4 in the baseline condition. The Insertion event in the baseline condition with FP1 and F4 showed N2, T3 had a P2 feature, and P4 had a P300 feature, while the MR condition had P300 at C3 and P2 at P3 and T5. The observed P2, N2, and P300 modulations remained significant after FDR correction across different electrodes and time windows ($q < 0.05$).

6. Discussion

6.1. Why using simulation?

We decided to use the MR simulation method, and specifically the opening of the blind product, stems from the undesirable results we got with inertial sensing gloves. With the arm as a positioning reference, superimposed on inertial offsets, errors remain unacceptable in blind assembly visualization that requires continuous operation. Whereas using external force sensors, pressure sensors do not face these challenges, so we wanted to bypass this difficulty with the existing hardware.

The use of cut-away perspective drawings is a basic approach in the teaching activities of blind assembly, or in the structural or process design phase, so we applied the idea of CAD drawings or 3D model drawings in perspective to the physical arrangement of the blind assembly. This is not realistic, but it achieves us excellent performance. However, it is not simply a matter of using the pass-through functionality of the MR HMD to copy the physical FoV. Products, parts and hands must be tracked and displayed in their entirety as prominent virtual models, ensuring that the essence of the simulation is not lost and the need for MR visualization is exceeded.

Furthermore, we acknowledge that a difference exists in the background environments between the MR and baseline conditions. In the baseline condition, participants directly viewed the real environment, whereas in the MR condition, they perceived it through a video pass-through feed. Although we employed a counter-balanced experimental order to mitigate learning effects, this environmental difference could potentially act as a confounding factor. The baseline condition provides a natural, unrestricted view of the real environment, while the MR condition presents the world through a video pass-through feed with a more limited FoV (89°). Secondly, the baseline condition include occlusion of the assembly scene by the opponent and parts, as well as occlusion of parts by the hand. In contrast, the MR condition rely on multi-modal methods such as force and haptic feedback, using virtual models as complete substitutes. However, we did not establish an additional MR blind assembly condition with occlusion. Because eliminating visual barriers and enhancing ergonomic freedom represent the cognitive benefits of in-situ visual guidance, and we aim to make predictions for future advanced equipment.

The core variable we intended to study was the difference in visual information presentation: the baseline condition forces reliance on mental reconstruction and tactile feedback, whereas the MR condition provides direct, unambiguous visual guidance. While the fidelity of the pass-through background differs from a direct real-world view, we argue that for the purposes of this task (e.g., seeing the bolts to be picked up), the functionality is comparable. Previous studies [64–66] on MR simulation have reached similar conclusions, namely that during focused tasks, the background environment does not exhibit a significant impact on users. Our analysis also primarily centered on the assembly phases of Pickup, Localization, and Insertion, during which cognitive processes are predominantly driven by interaction with the assembly product (virtual or occluded), rather than the peripheral background.

We verified that this simulated MR system can outperform current systems, at least in terms of having a positive effect on task performance, as well as having relatively better system ease of use. So hypotheses H1 and H2 are supported. The application of multiple sensors of the system also allows us to accurately monitor user behavior, ERP events rely on force and pressure sensor detection, which is not natively supported using inertial gloves. In summary, considering the hardware size, means of detection, accuracy, and the ability to discover more instructive kinetic reasons for MR visualization, we believe that the simulated visualization system is capable of making recommendations.

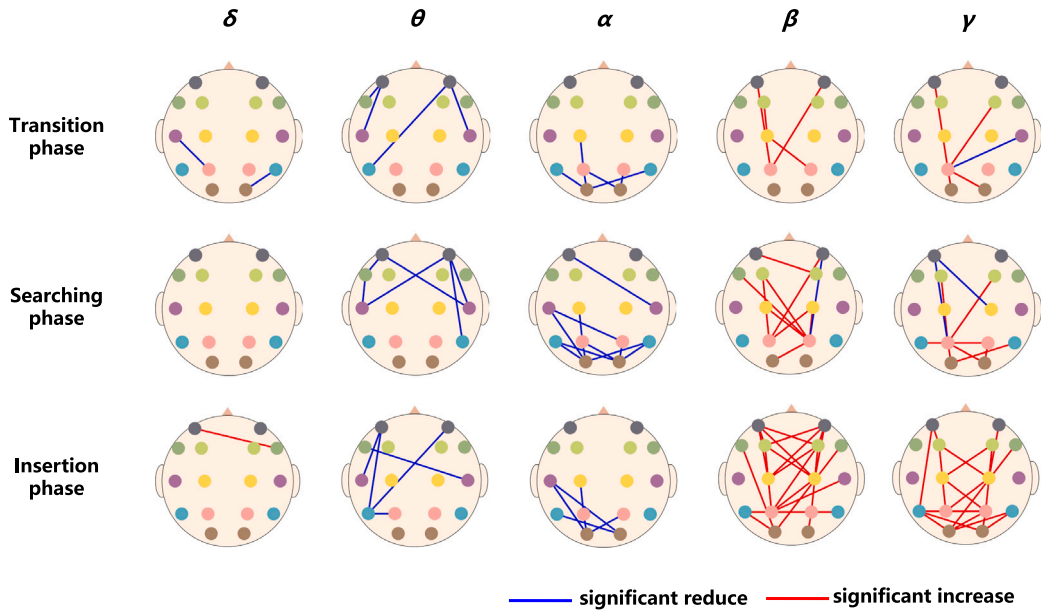

Fig. 11. Significant differences in Coh for the MR visualization condition relative to the blind assembly condition. ($P < 0.01$).

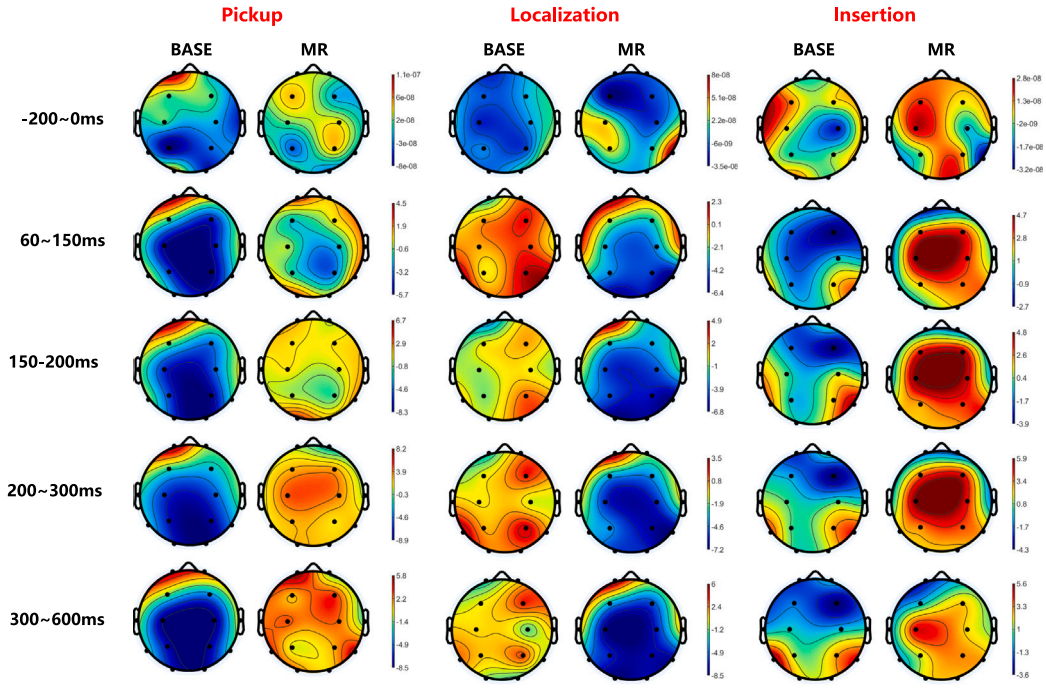

Fig. 12. The average topography of the trigger events.

6.2. MR visualization vs. Blind assembly

In this subsection, we analyze the effect of training condition on cognitive processing using EEG results, and the interview results.

Across all three phases, the θ power was significantly decreased in the prefrontal regions under the MR condition. The θ activity is widely associated with working memory [67] and attentional effort [68]. This reduction suggests that MR visualization reduces the need for participants to rely heavily on working memory, as the system provides real-time visual feedback of the assembly components and target locations. In contrast, blind assembly requires operators to mentally reconstruct [69] the task from paper instructions or tactile feedback, increasing cognitive load. Participants P2, P4, and P11 said, "Finding a target location based on a paper manual takes some time to think about". P8, and P10 said, "Although there is a 3D view that uses a perspective view, the paper document guidelines are not intuitive enough". Nearly half of the participants who responded to Q1 reported that it was subjectively easier to use the MR system.

During the searching and insertion phase, the γ power increased in the multi region under the MR condition. The γ oscillations are linked to enhanced visual processing [70], attention [71], and motor coordination [72]. These increases suggest that MR visualization more effectively engages the visual and motor systems, using superimposed virtual models to improve perception and facilitate precise action advantages compared to in the baseline condition where operators rely on non-visual cues. Participants P1, P8, P10, P16 all refer to seeing a direct

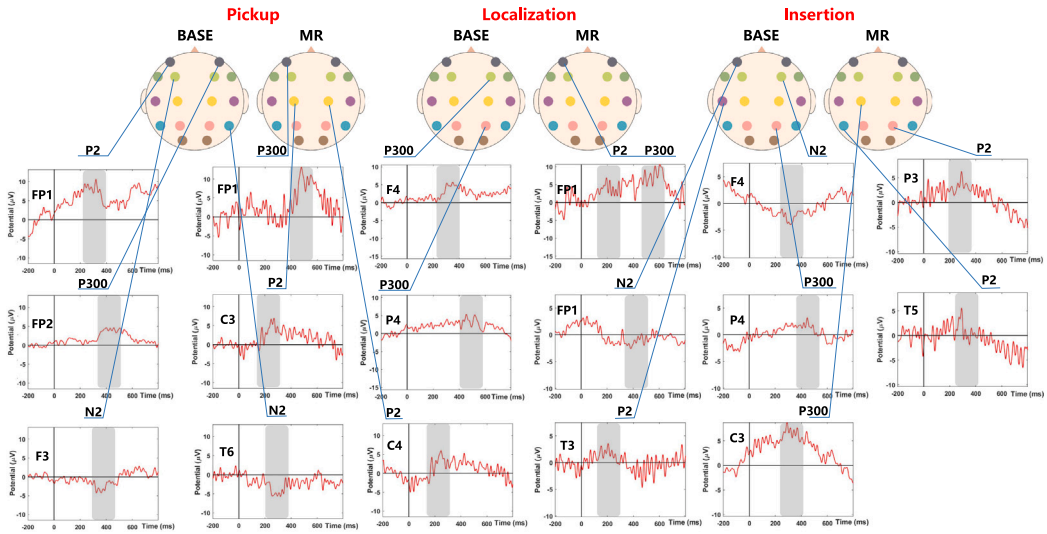

Fig. 13. Typical ERP components identified.

schematic of the target position in the MR visualization, which allows the hand to be moved quickly to the correct position. P18 stated that, "in the blind assembly, it is not at all clear where one's hand is until it is subjected to haptic feedback". It is clear that MR visualization provides support for precise action, and in addition to being able to see, more than 1/3 of the responses to Q2 mentioned that the errors and delays between the virtual and real models were small enough to give them sufficient confidence.

In the transition phase, decreased θ power in the prefrontal and inferior frontal regions alongside increased β power in the parietal region suggests a shift from effortful planning to visually guided preparation with MR support [72,73]. The searching phase's decrease in α power across multiple regions further implies reduced inhibition and heightened engagement with the visual stimuli provided by MR, contrasting with the blind condition's reliance on internal spatial mapping. In their responses to Q6, none of the participants indicated that they were able to distinguish the different stages on their own, or that particular events had a sense of segmentation.

In the MR condition, connectivity in the θ and α bands decreased significantly. Specifically, θ connectivity dropped between the prefrontal lobe and lateral frontal/temporal regions, while α connectivity decreased between the occipital lobe and parietal/posterior temporal/central regions. Lower connectivity in these bands suggests a reduced need for widespread neural integration [74]. In blind assembly, participants must synthesize tactile and proprioceptive inputs with memorized instructions, necessitating greater inter-regional coordination. MR visualization, by providing direct visual input, simplifies this process, minimizing the cognitive effort required for sensory integration. Conversely, connectivity in the β and γ bands increased in the MR condition. The β connectivity rose between the frontal, parietal, and central regions, while γ connectivity increased between the parietal, occipital, and prefrontal regions. These patterns reflect enhanced synchronization for motor planning [75] and visual-motor integration [76], facilitated by the MR system's real-time guidance. This contrasts with the blind condition, where motor actions rely on less precise, non-visual feedback, leading to less coordinated neural activity.

The significant reduction in θ power [77] in prefrontal regions during all task phases and a reduction in θ and α band coherence, satisfy hypothesis H3, supporting a reduction in cognitive load and cognitive simplification.

In th baseline condition, the N2 and P300 components exhibited prolonged latencies during localization and insertion events. For example, during localization, electrodes F4 and P4 showed delayed positivity, and during insertion, electrodes T5 and T6 displayed extended N2 and P300 features. The N2 component is associated with cognitive control and attention [78], while P300 reflects stimulus evaluation [79] and decision-making [80]. These delays suggest that blind assembly requires more time for sensory processing and decision-making, as participants rely on contact feedback to confirm positions without visual cues. In contrast, the MR condition showed shorter latencies for these components. For instance, during localization, FP1 exhibited rapid P2 and P300 responses, and during insertion, C3 and P3 showed prompt P300 and P2 features. These quicker responses indicate that visual feedback accelerates cognitive processing, allowing participants to evaluate stimuli and make decisions more efficiently. The immediate visibility of virtual models reduces uncertainty, streamlining the neural processes involved. This provides insights into H4, where events of haptic-visual integration have a significant effect on the modulation of cognitive resources.

The EEG characteristics of the blind assembly were similar to what we expected, a movement of motor imagery and haptic integration. MR visualization significantly improved the user experience through providing visual feedback, but unlike performing assembly operations in the real world, a stronger visual stimulus was given through the virtual model. Our two-condition comparison study differs from previous cognitive studies on virtual movements in that participants never see their hands directly, because participants do not train in open-ended products. Previous related work focused on comparing the differences between the virtual and the real.

There was more subjective feedback from the participants providing insights into the details. P2 said, "If the model is the same skin color as your own hand or translucent, you can focus more on the task, but the bolts being more prominent does benefit efficiency". P6 said, "The force feedback visualization of the bolt requires me to touch it in a fixed position, which is not very flexible but coherent, and would be more practical if I could also visualize tools such as wrenches for manipulation". P15 said, "The background environments are very immersive to me via pass-through replication, but the bolts are modeled at a slightly different size than reality, which can cause misinterpretation in fine manipulation". While the feedback was largely positive, some challenges were noted. Participants mentioned potential technical issues or discomfort with the MR headset.

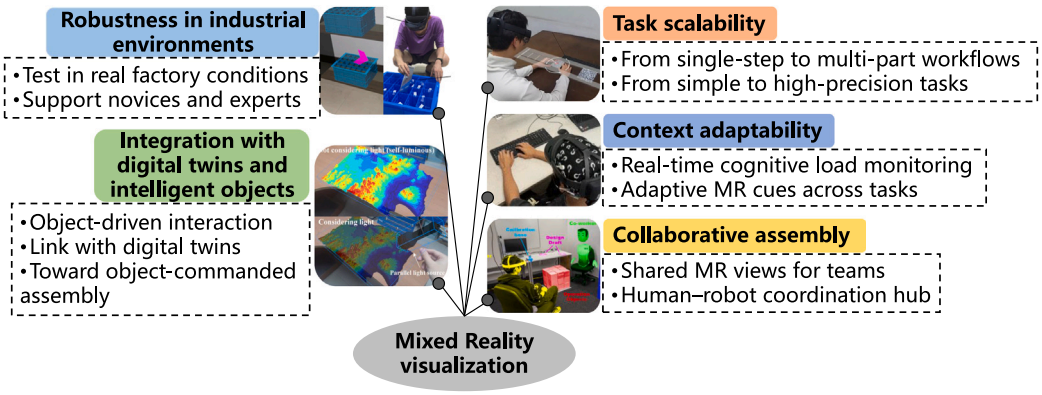

Fig. 14. The development roadmap for MR visualization systems.

6.3. Limitations and future work

Our "open box" approach intentionally circumvents existing hardware limitations. While exploring the core cognitive dynamics of an idealized visualization system, we must acknowledge the gap between controlled experimental environments and the challenges of real-world industrial deployment. This chapter explores the challenges of translating this concept into a practical tool for physically constrained, on-site assembly tasks and proposes potential strategies for future research

The primary and most critical challenge lies in tracking and registration within occluded spaces. Our configuration allows for reliable, inside-out optical tracking using the HMD's camera, as the hand and components are always within the FoV. However, in real-world blind assembly tasks, such as working inside a machine chassis, these optical systems fail due to physical obstructions. While alternative solutions exist, such as IMU-based gloves, they suffer from cumulative drift and require frequent recalibration. Another option is magnetic tracking, but this is generally unsuitable for industrial environments due to interference from surrounding metal structures. Therefore, a hybrid tracking system should be developed that intelligently fuses data from multiple sources, for example, combining an integrated IMU in the glove for high-frequency motion tracking with a miniature camera mounted on the tool for local visual feature-based correction, thus maintaining accuracy even when direct line of sight is lost.

The second challenge lies in the miniaturization and practical integration of the sensors. Our prototype uses 6-axis force and wired pressure sensors for accurate event detection. While this setup is effective for data acquisition, its bulkiness, wired connections, and fragility may hinder natural worker movements and workflow, making it difficult for industrial deployment. The solution lies in integrating miniaturized wireless sensing technology. The advancement of micro-electromechanical systems has enabled the development of compact, low-power force and pressure sensors. These can be directly embedded into the fingertips of ergonomic smart gloves or integrated into the assembly tools themselves, wirelessly transmitting data to HMDs or local controller via protocols such as low-energy Bluetooth.

Finally, deployment depends on the form factor and computing architecture of the HMD. Our research used a consumer-grade HMD connected to a laptop. An industrial solution must be a standalone, robust, and ergonomically designed device suitable for extended use. The computational load of real-time rendering of complex CAD models, coupled with running sophisticated sensor fusion algorithms, conflicts with the power and thermal limitations of lightweight, untethered devices. A promising approach to addressing this trade-off is edge computing or a split rendering architecture. In this model, the HMD remains lightweight, handling only the final rendering and local sensor communication. Heavy computational tasks (processing large models and running tracking algorithms) are offloaded to a powerful edge server in the factory environment, and the generated visual data is streamed wirelessly to the HMD. This approach enables a seamless, low-latency experience without compromising the ergonomics of the wearable device.

The insights gained can be translated into practical assembly environments. For example, cognitive metrics derived from EEG can guide the design of adaptive MR interfaces, dynamically adjusting visualization complexity based on the operator's cognitive load. Furthermore, identified behavioral correlations can inform ergonomic adjustments and task prioritization strategies in smart workshops, thereby achieving closed-loop optimization between cognitive feedback and process performance. As outlined in Fig. 14, we introduce on how to systematically expand, refine, and validate the cognitive and behavioral advantages demonstrated in our research, paving the way for MR systems that go beyond simple blind assembly tasks, supporting a wide range of complex, collaborative, and real-world industrial assembly applications.

While the present work focuses on offline cognitive analysis, the proposed event-driven and phase-aware framework provides a foundation for future methodological extensions. One promising direction is the integration of neuromuscular stimulation techniques, to actively support motor execution and proprioceptive feedback. Moreover, this framework may support the development of predictive or closed-loop assembly assistance strategies. These directions highlight the extensibility of the proposed framework and are beyond the scope of the current study.

7. Conclusions

This study presents an MR-simulated visualization system for blind-area assembly and examines its effects on brain activity and assembly performance through EEG analysis and a controlled user study with 24 participants. From both a practical manufacturing and methodological perspective, the findings provide actionable insights for MR-assisted assembly by explicitly aligning neural analysis with task-specific interaction events. The proposed phase-aware framework interprets EEG features across distinct assembly stages, revealing reduced cognitive load, faster neural responses, and improved task performance. These results indicate that MR visualization can effectively compensate for limited visual access in confined assembly spaces and should prioritize continuous spatial guidance, low-latency feedback, and event-aligned interaction cues to support critical stages such as localization and insertion. Fig. 15 shows the conclusions and application pathways.

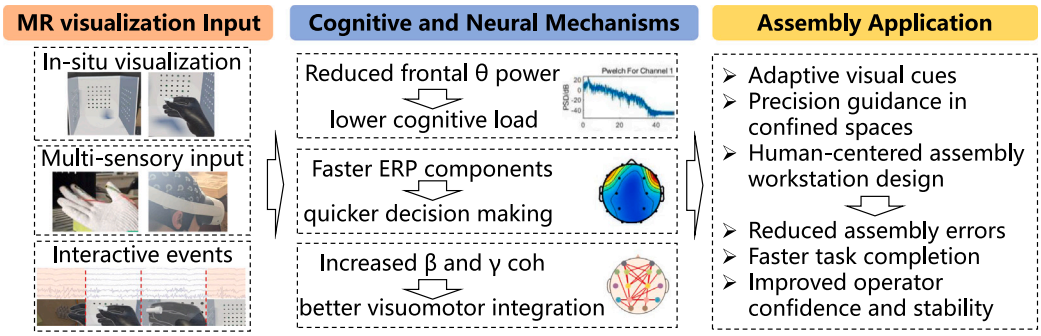

Fig. 15. The conclusions and application pathways.

Based on these results we propose the following design recommendations for the construction of MR visualization systems for blind assembly:

1. Optimize the allocation of cognitive resources. The observed reduction in frontal θ power and α desynchronization in MR condition, together with lower NASA-TLX mental demand scores, suggest that MR reduces the need for effortful mental reconstruction. Therefore, when designing a MR interface, it is important to provide continuous spatial cues (such as real-time highlighting of target locations) to reduce the user's reliance on spatial imagination and to avoid making the interface overly complex (for example, by highlighting key locations and hiding unnecessary elements).

2. Enhance sensorimotor integration. The ERP results showed earlier and more pronounced P2/P300 components in MR condition, indicating facilitated stimulus evaluation and decision-making. Therefore, it is essential to ensure high-precision, low-latency visual rendering, accurate matching of virtual models, hand movements, and assembly components, and integrate predictive visual cues, such as displaying target locations in advance, to accelerate decision-making.

3. Support user-centered adaptability. Differences in γ and β coherence across regions revealed that MR enhances functional connectivity associated with motor control and planning. This suggests that the adaptability of visualizations (e.g., adjustable levels of detail between schematic diagrams and full models to cater to individual preferences) can better meet users' ever-changing cognitive and motor needs.

4. Use multi-sensory channel fusion to provide feedback. Reduced frustration scores and fewer errors under MR, combined with enhanced parietal–occipital γ connectivity, point to more effective integration of visual and proprioceptive cues. The system should provide consistent multi-sensory feedback, such as a brief vibration or force feedback when parts are correctly aligned, which can reduce cognitive dissonance and improve operational accuracy.

CRediT authorship contribution statement

Tianyu Liu: Writing – review & editing, Writing – original draft, Visualization, Validation, Supervision, Software, Resources, Project administration, Methodology, Investigation, Funding acquisition, Formal analysis, Data curation, Conceptualization. **Weiping He:** Writing – review & editing, Funding acquisition. **Bokai Zheng:** Software, Methodology, Conceptualization. **Jilong Bai:** Software, Methodology, Conceptualization. **Xiaotian Zhang:** Software, Methodology, Conceptualization. **Wenbo Pang:** Software. **Yanli He:** Writing – review & editing, Funding acquisition. **Mark Billinghurst:** Writing – review & editing. **Lili Wang:** Writing – review & editing.

Declaration of generative AI and AI-assisted technologies in the manuscript preparation process

During the preparation of this work the authors used GPT-5 in order to improve language expression. After using this tool/service, the authors reviewed and edited the content as needed and take full responsibility for the content of the published article.

Declaration of competing interest

The authors declare that they have no known competing financial interests or personal relationships that could have appeared to influence the work reported in this paper.

Acknowledgments

This research was financially sponsored by the National Key R&D Program of China [Grant No. 2024YFB3311201]. We would like to thank the anonymous reviewers for their constructive suggestions for enhancing this paper.

Appendix A. Supplementary data

Supplementary material related to this article can be found online at https://doi.org/10.1016/j.jmsy.2026.02.018.

References

[1] Di Pasquale V, Miranda S, Neumann WP, Setayesh A. Human reliability in manual assembly systems: a Systematic Literature Review. Ifac-Papersonline 2018;51(11):675–80.
[2] Wang Z, Yan Y, Han D, Bai X, Zhang S. Product blind area assembly method based on augmented reality and machine vision. Xibei Gongye Daxue Xuebao/J Northwest Polytech Univ 2019;37(3):496–502.
[3] Wang Z, Bai X, Zhang S, Billinghurst M, He W, Wang P, Lan W, Min H, Chen Y. A comprehensive review of augmented reality-based instruction in manual assembly, training and repair. Robot Comput-Integr Manuf 2022;78:102407.
[4] Feng S, He W, Zhang S, Billinghurst M. Seeing is believing: AR-assisted blind area assembly to support hand–eye coordination. Int J Adv Manuf Technol 2022;119(11):8149–58.
[5] Zhang S, He W, Wang S, Feng S, Hou Z, Hu Y. An AR-enabled see-through system for vision blind areas. In: International conference on human-computer interaction. Springer; 2021, p. 206–13.
[6] Zhang X, He W, Bai J, Billinghurst M, Liu D, Dong J, Qin Y, Liu T, Wang Z. Integrate augmented reality and force sensing devices to assist blind area assembly. J Manuf Syst 2024;74:594–605.
[7] Wang Z, Zhou Y, Xiong F, Xiao J, Lu R, Han F. Visual encoding method for MR interface operation process prompts Supporting Blind Area assembly. In: 2024 IEEE 2nd international conference on control, electronics and computer technology. IEEE; 2024, p. 113–7.
[8] Hou Z, Zhang Q, Wang S, He W, Zhang S. A blind area information perception and AR assembly guidance method based on RGBD data for dynamic environments and user study. Int J Adv Manuf Technol 2024;133(1):115–28.
[9] Dargar S, Kennedy R, Lai W, Arikatla V, De S. Towards immersive virtual reality (iVR): a route to surgical expertise. J Comput Surg 2015;2:1–26.
[10] Dalle Mura M, Dini G, Failli F. An integrated environment based on augmented reality and sensing device for manual assembly workstations. Procedia Cirp 2016;41:340–5.
[11] Lee C, Bonebrake S, Bowman DA, Höllerer T. The role of latency in the validity of AR simulation. In: 2010 IEEE virtual reality conference. IEEE; 2010, p. 11–8.
[12] Kober SE, Settgast V, Brunnhofer M, Augsdörfer U, Wood G. Move your virtual body: differences and similarities in brain activation patterns during hand movements in real world and virtual reality. Virtual Real 2022;1–11.
[13] Karamians R, Proffitt R, Kline D, Gauthier LV. Effectiveness of virtual reality- and gaming-based interventions for upper extremity rehabilitation poststroke: a meta-analysis. Arch Phys Med Rehabil 2020;101(5):885–96.

[14] Laver KE, Lange B, George S, Deutsch JE, Saposnik G, Crotty M. Virtual reality for stroke rehabilitation. Cochrane Database Syst Rev 2017;(11).
[15] Reynolds C, Osuagwu BA, Vuckovic A. Influence of motor imagination on cortical activation during functional electrical stimulation. Clin Neurophysiol 2015;126(7):1360–9.
[16] Wang Z, Zhang S, Bai X. Augmented reality based product invisible area assembly assistance. In: 2018 3rd international conference on control, automation and artificial intelligence. Atlantis Press; 2018, p. 109–13.
[17] Khenak N, Vézien J, Bourdot P. Effectiveness of augmented reality guides for blind insertion tasks. Front Virtual Real 2020;1:588217.
[18] Chu C-H, Ko C-H. An experimental study on augmented reality assisted manual assembly with occluded components. J Manuf Syst 2021;61:685–95.
[19] Fang W, Hong J. Bare-hand gesture occlusion-aware interactive augmented reality assembly. J Manuf Syst 2022;65:169–79.
[20] Zheng Y, Li Y, Wu W, Meng F, Chen C. Visual guidance method for artificial assembly in visual blind areas based on augmented reality. Int J Adv Manuf Technol 2024;134(1):969–85.
[21] Kumar N, Kumar J. Measurement of cognitive load in HCI systems using EEG power spectrum: an experimental study. Procedia Comput Sci 2016;84:70–8.
[22] Frey J, Daniel M, Castet J, Hachet M, Lotte F. Framework for electroencephalography-based evaluation of user experience. In: Proceedings of the 2016 CHI conference on human factors in computing systems. 2016, p. 2283–94.
[23] Hosseini SA, Khalilzadeh MA. Emotional stress recognition system using EEG and psychophysiological signals: Using new labelling process of EEG signals in emotional stress state. In: 2010 international conference on biomedical engineering and computer science. IEEE; 2010, p. 1–6.
[24] Saffaryazdi N, Goonesekera Y, Saffaryazdi N, Hailemariam ND, Temesgen EG, Nanayakkara S, Broadbent E, Billinghurst M. Emotion recognition in conversations using brain and physiological signals. In: Proceedings of the 27th international conference on intelligent user interfaces. 2022, p. 229–42.
[25] Lee HS, Park YJ, Park SW. The effects of virtual reality training on function in chronic stroke patients: a systematic review and meta-analysis. BioMed Res Int 2019;2019(1):7595639.
[26] Adamovich SV, Fluet GG, Tunik E, Merians AS. Sensorimotor training in virtual reality: a review. NeuroRehabilitation 2009;25(1):29–44.
[27] Graziano MS, Gross CG. Visual responses with and without fixation: neurons in premotor cortex encode spatial locations independently of eye position. Exp Brain Res 1998;118:373–80.
[28] Hadipour-Niktarash A, Lee CK, Desmond JE, Shadmehr R. Impairment of retention but not acquisition of a visuomotor skill through time-dependent disruption of primary motor cortex. J Neurosci 2007;27(49):13413–9.
[29] Muellbacher W, Ziemann U, Boroojerdi B, Cohen L, Hallett M. Role of the human motor cortex in rapid motor learning. Exp Brain Res 2001;136:431–8.
[30] Perani D, Fazio F, Borghese NA, Tettamanti M, Ferrari S, Decety J, Gilardi MC. Different brain correlates for watching real and virtual hand actions. Neuroimage 2001;14(3):749–58.
[31] Perez-Marcos D, Slater M, Sanchez-Vives MV. Inducing a virtual hand ownership illusion through a brain–computer interface. Neuroreport 2009;20(6):589–94.
[32] González-Franco M, Peck TC, Rodríguez-Fornells A, Slater M. A threat to a virtual hand elicits motor cortex activation. Exp Brain Res 2014;232(3):875–87.
[33] Alimardani M, Nishio S, Ishiguro H. Brain-computer interface and motor imagery training: The role of visual feedback and embodiment. In: Evolving BCI therapy-engaging brain state dynamics. IntechOpen; 2018.
[34] Kober SE, Settgast V, Brunnhofer M, Augsdörfer U, Wood G. Move your virtual body: differences and similarities in brain activation patterns during hand movements in real world and virtual reality. Virtual Real 2022;1–11.
[35] Tieri G, Tidoni E, Pavone EF, Aglioti SM. Mere observation of body discontinuity affects perceived ownership and vicarious agency over a virtual hand. Exp Brain Res 2015;233:1247–59.
[36] Argelaguet F, Hoyet L, Trico M, Lécuyer A. The role of interaction in virtual embodiment: Effects of the virtual hand representation. In: 2016 IEEE virtual reality. IEEE; 2016, p. 3–10.
[37] Singh AK, Gramann K, Chen H-T, Lin C-T. The impact of hand movement velocity on cognitive conflict processing in a 3D object selection task in virtual reality. NeuroImage 2021;226:117578.
[38] Schwind V, Lin L, Di Luca M, Jörg S, Hillis J. Touch with foreign hands: The effect of virtual hand appearance on visual-haptic integration. In: Proceedings of the 15th ACM symposium on applied perception. 2018, p. 1–8.
[39] Xiao H, Duan Y, Zhang Z, Li M. Detection and estimation of mental fatigue in manual assembly process of complex products. Assem Autom 2018;38(2):239–47.
[40] Kosch T, Funk M, Schmidt A, Chuang LL. Identifying cognitive assistance with mobile electroencephalography: A case study with in-situ projections for manual assembly. Proc ACM Human-Comput Interact 2018;2(EICS):1–20.
[41] Pušica M, Caiazzo C, Djapan M, Savković M, Leva MC. Visual mental workload assessment from EEG in manual assembly task. In: Proceedings of the 33rd European safety and reliability conference. southampton, UK; 2023, p. 3–7.
[42] Qin Y, Bulbul T. An EEG-based mental workload evaluation for AR head-mounted display use in construction assembly tasks. J Constr Eng Manag 2023;149(9):04023088.
[43] Qin Y, Bulbul T. Electroencephalogram-based mental workload prediction for using augmented reality head mounted display in construction assembly: A deep learning approach. Autom Constr 2023;152:104892.
[44] Qin Y, Bulbul T, Withers J. EEG-based classification of cognitive load and task conditions for AR supported construction assembly: A deep learning approach. In: Computing in civil engineering 2023. 2023, p. 248–56.
[45] Morton J, Zheleva A, Van Acker BB, Durnez W, Vanneste P, Larmuseau C, De Bruyne J, Raes A, Cornillie F, Saldien J, et al. Danger, high voltage! using EEG and EOG measurements for cognitive overload detection in a simulated industrial context. Appl Ergon 2022;102:103763.
[46] Alessa FM, Alhaag MH, Al-Harkan IM, Ramadan MZ, Alqahtani FM. A neurophysiological evaluation of cognitive load during augmented reality interactions in various industrial maintenance and assembly tasks. Sensors 2023;23(18):7698.
[47] Mijović P, Ković V, De Vos M, Mačužić I, Jeremić B, Gligorijević I. Benefits of instructed responding in manual assembly tasks: an ERP approach. Front Hum Neurosci 2016;10:171.
[48] Mohammed A, Wang L. Brainwaves driven human-robot collaborative assembly. CIRP Ann 2018;67(1):13–6.
[49] Mohammed A, Wang L. Advanced human-robot collaborative assembly using electroencephalogram signals of human brains. Procedia CIRP 2020;93:1200–5.
[50] Mohammed A, Wang L. Intelligent human–robot assembly enabled by brain EEG. In: Advanced human-robot collaboration in manufacturing. Springer; 2021, p. 351–71.
[51] Buerkle A, Bamber T, Lohse N, Ferreira P. Feasibility of detecting potential emergencies in symbiotic human-robot collaboration with a mobile EEG. Robot Comput-Integr Manuf 2021;72:102179.
[52] Buerkle A, Eaton W, Lohse N, Bamber T, Ferreira P. EEG based arm movement intention recognition towards enhanced safety in symbiotic Human-Robot Collaboration. Robot Comput-Integr Manuf 2021;70:102137.
[53] Wang L, Liu S, Cooper C, Wang XV, Gao RX. Function block-based human-robot collaborative assembly driven by brainwaves. CIRP Ann 2021;70(1):5–8.
[54] Lahoud F, Susstrunk S. Ar in vr: Simulating infrared augmented vision. In: 2018 25th IEEE international conference on image processing. IEEE; 2018, p. 3893–7.
[55] Tran TTM, Parker C, Hoggenmüller M, Hespanhol L, Tomitsch M. Simulating wearable urban augmented reality experiences in vr: Lessons learnt from designing two future urban interfaces. Multimodal Technol Interact 2023;7(2):21.
[56] Dufresne F, Nilsson T, Gorisse G, Guerra E, Zenner A, Christmann O, Bensch L, Callus NA, Cowley A. Touching the moon: leveraging passive haptics, embodiment and presence for operational assessments in virtual reality. In: Proceedings of the 2024 CHI conference on human factors in computing systems. 2024, p. 1–18.
[57] Meta. Meta quest 3S. 2025, URL https://www.meta.com/sg/quest/quest-3s/.
[58] DST(Shenzhen) Sensing System Engineering CoLtd. γ74-DECENT. 2022, URL http://dstcgq.com/en/sixxaxisxforcexsensor/11.html.
[59] neuracle. NeuSen W wireless EEG acquisition system. 2025, URL http://www.neuracle.cn/productinfo/148706.html.
[60] Unity Technologies. Meta XR all-in-one SDK. 2025, URL http://dstcgq.com/en/sixxaxisxforcexsensor/11.html.
[61] Saghalaini M, Ghanbari Z, Moradi MH. Applying B-value and empirical equivalence hypothesis testing to intellectual and developmental disabilities electroencephalogram data. In: Signal processing with python: a practical approach. IOP Publishing Bristol, UK; 2024, p. 1–2.
[62] Picton TW, Bentin S, Berg P, Donchin E, Hillyard SA, Johnson R, Miller GA, Ritter W, Ruchkin DS, Rugg MD, et al. Guidelines for using human event-related potentials to study cognition: recording standards and publication criteria. Psychophysiology 2000;37(2):127–52.
[63] Luck SJ. An introduction to the event-related potential technique. MIT Press; 2014.
[64] Lee C, Bonebrake S, Hollerer T, Bowman DA. A replication study testing the validity of AR simulation in VR for controlled experiments. In: 2009 8th IEEE international symposium on mixed and augmented reality. 2009, p. 203–4. http://dx.doi.org/10.1109/ISMAR.2009.5336464.
[65] Lahoud F, Susstrunk S. Ar in VR: Simulating Infrared Augmented Vision. In: 2018 25th IEEE international conference on image processing. 2018, p. 3893–7. http://dx.doi.org/10.1109/ICIP.2018.8451811.
[66] Liu T, He W, Billinghurst M. Assessing the effectiveness of mixed reality as a simulation tool for augmented reality office applications. IEEE Trans Vis Comput Graphics 2025;31(10):9092–103. http://dx.doi.org/10.1109/TVCG.2025.3590002.
[67] Jensen O, Tesche CD. Frontal theta activity in humans increases with memory load in a working memory task. Eur J Neurosci 2002;15(8):1395–9.
[68] Landau AN, Schreyer HM, Van Pelt S, Fries P. Distributed attention is implemented through theta-rhythmic gamma modulation. Curr Biol 2015;25(17):2332–7.
[69] Kalyuga S. Knowledge elaboration: A cognitive load perspective. Learn Instr 2009;19(5):402–10.
[70] Müller MM, Gruber T, Keil A. Modulation of induced gamma band activity in the human EEG by attention and visual information processing. Int J Psychophysiol 2000;38(3):283–99.

[71] Jensen O, Kaiser J, Lachaux J-P. Human gamma-frequency oscillations associated with attention and memory. Trends Neurosci 2007;30(7):317–24.
[72] Ulloa JL. The control of movements via motor gamma oscillations. Front Hum Neurosci 2022;15:787157.
[73] Wróbel A. Beta activity: a carrier for visual attention. Acta Neurobiol Exp 2000;60(2):247–60.
[74] Waldhauser GT, Johansson M, Hanslmayr S. Alpha/beta oscillations indicate inhibition of interfering visual memories. J Neurosci 2012;32(6):1953–61.
[75] Ewen JB, Lakshmanan BM, Hallett M, Mostofsky SH, Crone NE, Korzeniewska A. Dynamics of functional and effective connectivity within human cortical motor control networks. Clin Neurophysiol 2015;126(5):987–96.
[76] Wang W, Li H, Wang Y, Liu L, Qian Q. Changes in effective connectivity during the visual-motor integration tasks: a preliminary f-NIRS study. Behav Brain Funct 2024;20(1):4.
[77] Antonenko P, Paas F, Grabner R, Van Gog T. Using electroencephalography to measure cognitive load. Educ Psychol Rev 2010;22:425–38.
[78] Folstein JR, Van Petten C. Influence of cognitive control and mismatch on the N2 component of the ERP: a review. Psychophysiology 2008;45(1):152–70.
[79] Magliero A, Bashore TR, Coles MG, Donchin E. On the dependence of P300 latency on stimulus evaluation processes. Psychophysiology 1984;21(2):171–86.
[80] Mansor AA, Isa SM, Noor SSM. P300 and decision-making in neuromarketing. Neurosci Res Notes 2021;4(3):21–6.